Dalton Transactions

Reactivity differences in the cyclometalation properties of bisphosphinimine-supported organo-rare earth complexes

Journal:	*Dalton Transactions*
Manuscript ID:	DT-ART-03-2014-000863.R1
Article Type:	Paper
Date Submitted by the Author:	30-Apr-2014
Complete List of Authors:	Zamora, Matthew; University of Lethbridge, Chemistry and Biochemistry Johnson, Kevin; University of Lethbridge, Chemistry and Biochemistry Hänninen, Mikko; University of Lethbridge, Chemistry and Biochemistry Hayes, Paul; University of Lethbridge, Chemistry and Biochemistry

Dalton Transactions

RSCPublishing

ARTICLE

Differences in the cyclometalation reactivity of bisphosphinimine-supported organo-rare earth complexes

Cite this: DOI: 10.1039/x0xx00000x

Matthew T. Zamora, Kevin R. D. Johnson, Mikko M. Hänninen, and Paul G. Hayes*

Received 00th March 2014,
Accepted 00th April 2014

DOI: 10.1039/x0xx00000x

www.rsc.org/

The pyrrole-based ligand *N*,*N*'-((1*H*-pyrrole-2,5-diyl)bis(diphenylphosphoranylylidene))bis(4-*iso*propylaniline) (H$\mathbf{L_B}$) can be deprotonated and coordinated to yttrium and samarium ions upon reaction with their respective trialkyl precursors. In the case of yttrium, the resulting complex [$\mathbf{L_B}$Y(CH_2SiMe_3)$_2$] (**1**) is a Lewis base-free monomer that is remarkably resistant to cyclometalation. Conversely, the analogous samarium complex [$\mathbf{L_B}$Sm(CH_2SiMe_3)$_2$] is dramatically more reactive and undergoes rapid *ortho*metalation of one phosphinimine aryl substituent, generating an unusual 4-membered azasamaracyclic THF adduct [κ^4-$\mathbf{L_B}$Sm(CH_2SiMe_3)(THF)$_2$] (**2**). This species undergoes further transformation in solution to generate a new dinuclear species that features unique carbon and nitrogen bridging units [κ^1:κ^2:μ^2-$\mathbf{L_B}$Sm(THF)]$_2$ (**3**). Alternatively, if **2** is intercepted by a second equivalent of H$\mathbf{L_B}$, the doubly-ligated samarium complex [(κ^4-$\mathbf{L_B}$)$\mathbf{L_B}$Sm] **(4)** forms.

Introduction

The organometallic chemistry of trivalent rare earth complexes has found many important applications in the field of catalysis, including the metal-catalyzed hydrophosphonylation of carbonyls,[1] hydrogenation,[2-7] the catalytic addition of H–X to unsaturated moieties (*e.g.* hydroamination,[8-16] hydrosilylation,[10, 16-20] hydrophosphination,[21-24] hydroboration,[25, 26] and hydroalkoxylation,[27-30]), and especially polymerization chemistry.[31-44] However, compared to research on organotransition-metal species, the study of rare earth complexes remains much less explored. For instance, stabilization of rare earth organometallic complexes has traditionally focused on simple carbocyclic frameworks,[45] particularly cyclopentadienyl motifs. More contemporary studies have incorporated a broad array of tunable ligand scaffolds that can provide a plethora of different steric and electronic environments.[46, 47]

As a result, the development of new ancillary ligands to support stoichiometric and catalytic transformations at rare earth metal centres is an important and intensively studied area of organolanthanide chemistry.[31, 45, 47, 48] To this end, we have recently reported a variety of carbazole-based bisphosphinimine frameworks for supporting complexes of Sc, Y and Lu (Chart 1, H$\mathbf{L_A}$).[49-53] These ligands can be attached to rare earth metal centres *via* either an alkane elimination route or by a salt metathesis pathway.[53] Depending on the size of the metal, one or more molecules of coordinating solvent is occasionally required to fill the coordination sphere of the resulting complex and prevent further decomposition.

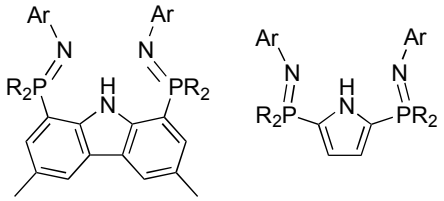

Chart 1 Carbazole (H$\mathbf{L_A}$) and pyrrole (H$\mathbf{L_B}$) bisphosphinimine proteo ligands.

We are highly interested in monitoring the metalation reactivity of these bisphosphinimine-ligated complexes owing to the ubiquitous nature of this process, especially in hydroelementation catalysis. Metalation is described frequently in modern literature, although generally as an undesirable ligand decomposition pathway. However, prior to 1960, only Group I metal alkyls were known to prominently convert sp^2 or sp^3 C–H bonds to a C–M bonded species. It was subsequently shown by Kaska, while under the supervision of Eisch,[54, 55] that metalative processes such as direct sp^2 C–H metalation could be facilitated by other organometallic species. Further pioneering work by Kaska demonstrated that even sp^3 C–H metalation could be promoted by intramolecular processes that use the entropically-driven attachment of a pincer ligand.[56] Over the decades that followed, the importance of the C–M bond has been realized in a multitude of molecular and materials applications that are intrinsically important to the future of sustainable catalysis. However, studies of C–H activation in the context of gaining the understanding required to rationally develop metalation-*resistant* ligands has served as the impetus for our studies in this area.

In our research focussed on rare earth complexes, we have observed that lanthanide alkyl derivatives supported by ligands of type **A** commonly undergo *several* C–H cyclometalation processes, however, these transformations often limit subsequent reactivity. For example, the lutetium complex [$\mathbf{L_A}$Lu(CH_2SiMe_3)$_2$] rapidly decomposes *via* two stepwise intramolecular cyclometalation reactions at ambient temperature (Scheme 1).[49] As a result, we initiated studies to generate a new set of ligands in an attempt to prepare more thermally robust rare earth metal complexes.

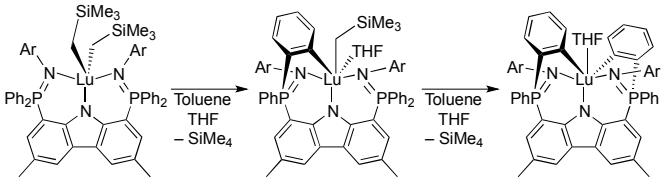

Scheme 1 Cyclometalative behaviour of a carbazole-based bisphosphinimine lutetium complex.

Accordingly, we designed a new pyrrole-based bisphosphinimine ligand (Chart 1, H$\mathbf{L_B}$) which, upon coordination to a variety of rare earth metals, yielded substantially more stable complexes, even when bearing substituents identical to the carbazole-based analogue.[57] More specifically, solutions of [$\mathbf{L_B}MR_2$] (M = Sc, Lu, Er) complexes are resistant to cyclometalation at elevated temperatures (60 °C for more than 4 h),[57] whereas **A**-type complexes immediately begin to convert into P- and/or N-aryl cyclometalated products at ambient temperature, despite the presence of coordinating solvent.[49, 50] Owing to the stabilizing effect of ligand $\mathbf{L_B}$, we became interested in expanding the study of this pyrrole-based ligand to include even larger rare earth metals. Our results are presented herein.

Results and Discussion

Yttrium Complex Synthesis and Stability

In contrast to transition metal chemistry, coordination numbers of organolanthanide complexes are heavily governed by the ionic radius of the encapsulated metal centre.[58, 59] Our previously reported organometallic complexes of $\mathbf{L_B}$ were of general form [$\mathbf{L_B}M(CH_2SiMe_3)_2$], (M = Sc, Lu and Er); these rare earth metals possess small ionic radii relative to the rest of the lanthanide series,[58] with the erbium congener being the largest of the three. Due to the fact that the erbium organometallic complex of $\mathbf{L_B}$ was found to be thermally robust, we were interested in exploring the stability of even larger rare earth ions. Hence, we targeted the preparation of an analogous complex of the slightly larger rare earth metal yttrium in order to establish whether C–H activation of the ligand substituents would prevail.

The yttrium complex **1** was prepared by reaction of [$Y(CH_2SiMe_3)_3(THF)_2$][60-62] with the proteo ligand H$\mathbf{L_B}$ (R = Ph, Ar = Pipp; Pipp = *para-iso*propylphenyl) in a pentane/THF solvent mixture at ambient temperature. Although [$Y(CH_2SiMe_3)_3(THF)_2$] can be isolated, it is thermally sensitive and **1** can also be obtained through an *in situ* alkane elimination process (Scheme 2).

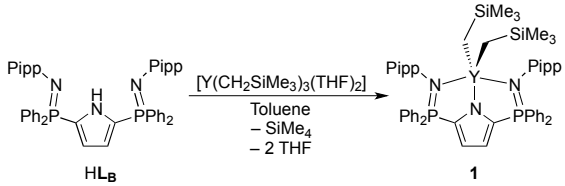

Scheme 2 Formation of pyrrole-based bisphosphinimine yttrium complex **1**.

Formation of complex **1** was evident by monitoring the reaction by multinuclear NMR spectroscopy. Specifically, in the $^{31}P\{^1H\}$ NMR spectrum, disappearance of the signal for free proteo ligand (δ –8.1) and concomitant emergence of one new signal further downfield at δ 25.0 with diagnostic splitting (d, $^2J_{P-Y}$ = 7.5 Hz; ^{89}Y = 100% abundant, I = ½) indicated that the ligand was coordinated to Y symmetrically *via* both phosphinimine donors. The ^1H NMR spectrum is also consistent with that expected for complex **1**, particularly, the presence of an upfield resonance at δ –0.04 which can be attributed to the four –CH_2SiMe$_3$ methylene protons. The pyrrole resonance is split into a doublet of doublets, due to coupling to two magnetically inequivalent ^{31}P nuclei (dd, $^3J_{H-P}$ = 2.1 Hz, $^4J_{H-P}$ = 1.2 Hz). As was observed with the previously reported Sc and Lu analogues, complex **1** contains no coordinated THF ligands, confirmed by the absence of THF resonances in the ^1H NMR spectrum; this is a notable feature considering that base-free, 5-coordinate yttrium complexes are relatively unusual. Finally, the $^{13}C\{^1H\}$ NMR spectrum closely matches those of related Lu and Sc complexes,[57] with the exception that this spectrum's CH_2 resonance exhibits the expected one-bond coupling to yttrium (d, $^1J_{C-Y}$ = 39 Hz).

Single crystals of **1** suitable for X-ray diffraction were readily obtained by slow diffusion of pentane into a concentrated toluene solution of **1** at –35 ºC. The molecular structure of **1** is depicted in Figure 1 as a thermal displacement plot. In the solid state, **1** is monomeric with the yttrium centre coordinated by two trimethylsilylmethyl groups and the tridentate pyrrole ligand bound by the three nitrogen atoms. The geometry is best described as distorted trigonal bipyramidal with the equatorial plane defined by N1 and the alkyl groups, while the bisphosphinimine donors (N2 and N3) occupy the apical sites. The bond angles about the equatorial plane are close to the ideal value of 120º (N1–Y1–C47 = 115.81(9)º, N1–Y1–C51 = 116.88(9)º, C51–Y1–C47 = 127.31(10)º); however, the apical bond angle deviates significantly from 180º (N2–Y1–N3 = 141.96(7)º). As a result, the structure bears a striking resemblance to its Lu and Er analogues.[57] Complex **1** exhibits Ln–C bond lengths (Y1–C47 = 2.412(3) Å, Y1–C51 = 2.394(3) Å) which fall within the range for typical Y–CH_2SiMe_3 bonds.[63] Additionally, these bond lengths are similar to those observed in the reported Er analogue (2.375(6) Å, 2.397(5) Å), and slightly longer than those found in the corresponding Lu congener (2.347(4) Å, 2.355(4) Å).[57]

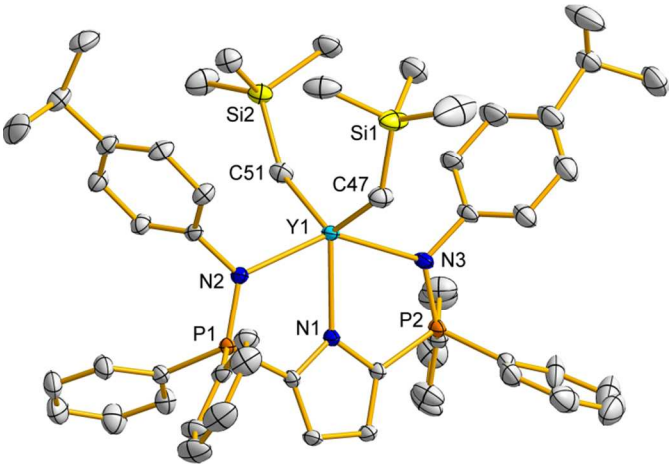

Figure 1. Thermal displacement plot (30% probability) of complex **1** with hydrogen atoms and minor disordered components omitted for clarity. Selected bond distances (Å) and angles (deg): P1–N2 = 1.6006(2), P2–N3 = 1.609(2), Y1–N1 = 2.345(2), Y1–N2 = 2.374(2), Y1–N3 = 2.410(2), Y1–C47 = 2.412(3), Y1–C51 = 2.393(4); C1–P1–N2 = 103.3(1), C4–P2–N3 = 104.2(1), C47–Y1–C51 = 127.3(1), N2–Y1–N3 = 141.97(8).

Since previously-reported rare earth (Sc, Lu, Er) dialkyl complexes ligated by $\mathbf{L_B}$ did not display evidence of intramolecular C–H activation,[57] we were interested in determining if the larger and more reactive yttrium metal centre in complex **1** would be prone to cyclometalation at either the phosphorus or nitrogen aryl substituents. Such a process would generate a 4- or 5-membered heteroyttricycle, depending on the site of C–H activation. However, similar to the previously-reported Sc, Lu and Er species, complex **1** is surprisingly resistant to cyclometalation, with no C–H activation occurring at either the phenyl substituents on phosphorus, or the nitrogen Pipp groups. More specifically, complex **1** has proven to be surprisingly robust, with no sign of cyclometalation even after several hours in solution (benzene-d_6) at ambient temperature.

Synthesis and Cyclometalation Reactivity of Organosamarium Derivatives

In the search for more reactive metals, we became intrigued by the unique reactivity of other lanthanide complexes. Samarium complexes were of particular interest, especially because of their utility in such processes as organic synthesis,[4] multifunctional asymmetric catalysis,[64] and hydroamination chemistry.[8] Furthermore, given the even larger ionic radius of samarium(III) relative to that of our previously described trivalent rare earth complexes of $\mathbf{L_B}$, we were curious as to whether complexes ligated by our new pyrrole-based bisphosphinimine ligand would remain inert to C–H activation, or if these species would succumb to cyclometalative transformations akin to our prior carbazole-based systems.

Rather than the expected dialkyl species **2'**, reaction of the proteo ligand H$\mathbf{L_B}$ with $[Sm(CH_2SiMe_3)_3(THF)_3]$[65] resulted in formation of the cyclometalated organosamarium product **2** (Scheme 3). Low overall reaction yields were obtained when the trialkyl samarium reagent was isolated prior to reaction with H$\mathbf{L_B}$, due to the fact that it rapidly decomposes at temperatures above –35 ºC. However, complex **2** was obtained in substantially higher yields when $[Sm(CH_2SiMe_3)_3(THF)_3]$ was prepared *in situ* by reaction of $[SmCl_3(THF)_2]$ with three equivalents of $LiCH_2SiMe_3$ in THF at –78 ºC, and subsequently reacted with a toluene solution of the proteo ligand.

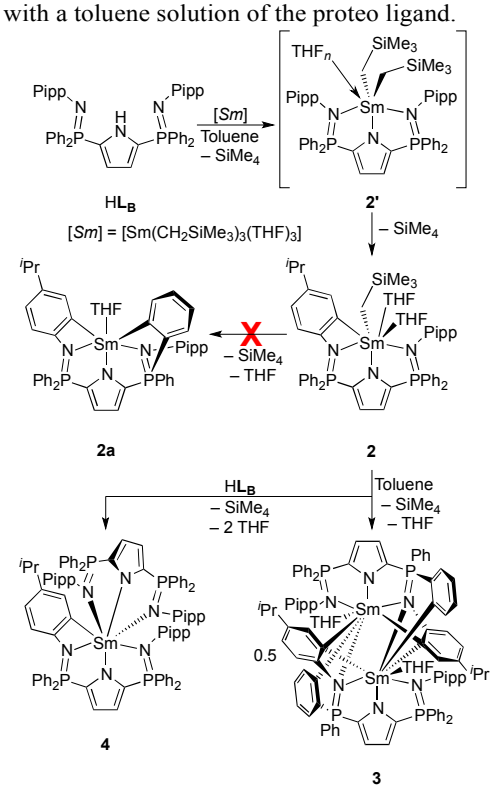

Scheme 3. Synthesis of bisphosphinimine-ligated samarium complexes.

The reaction leading to the formation of complex **2** most likely proceeds through the putative non-cyclometalated THF adduct (**2'**) that contains two trimethylsilylmethyl groups. However, efforts to isolate **2'** met with little success, a fact which was not surprising given that this species could not be observed spectroscopically, even at temperatures as low as –78 ºC in toluene-d_8. Presumably dialkyl **2'** is highly unstable and upon formation immediately undergoes cyclometalation of one of the ancillary ligand N-aryl rings to form the four-membered azasamaracycle **2**. Hence, the rate constant for decomposition of **2'** is likely larger than that of its formation. When the reaction was monitored spectroscopically in benzene-d_6, the $^{31}P\{^1H\}$ NMR resonance attributed to the free ligand H$\mathbf{L_B}$ (δ –8.1) disappeared as two new signals emerged at δ 24.5 and 18.1 in a 1:1 ratio. This ligand asymmetry was also observed in the ^1H NMR spectrum whereby several overlapping resonances afforded a much more complicated spectrum than would be expected for **2'**. For example, the two diagnostic doublets attributed to the N-aryl groups are both more complex than anticipated and each integrate to only 1H. Furthermore, four separate signals were observed for the ^{i}Pr methyl groups, which is more likely a result of asymmetry rather than restricted rotation about the C_{ipso}–CH bond. Notably, these NMR spectra are generally devoid of the features characteristic of strongly paramagnetic complexes: most signals exhibit relatively routine chemical shifts and the resonances are narrow with widths at half height (whh) in the range of those typically observed for diamagnetic compounds (2.0 Hz ≤ whh ≤ 3.4 Hz); however, some minor paramagnetic characteristics are also evident in the spectra. This phenomenon can be attributed to the relatively weak magnetic moment of samarium compared to most of the other trivalent lanthanides.[66]

High quality crystals of **2** were obtained from slow diffusion of pentane into a concentrated THF solution of **2** at –35 ºC. In the solid state, the heptacoordinate samarium complex **2** is defined by one trimethylsilylmethyl group, a tetradentate pyrrole ligand bound by the three expected nitrogen atoms as well as the *ortho* carbon of one phosphinimine N-Pipp substituent, and two *cis*-oriented THF solvent molecules (Figure 2). Complex **2** adopts a 7-coordinate geometry that is best described as pentagonal bipyramidal, with the alkyl ligand and one THF ligand residing in the apical sites. The equatorial positions about samarium do not deviate substantially from planarity, as indicated by the sum of the internal angles ($\sum_{\angle}$ = 358º). As expected, the THF ligand in the equatorial plane is bound more strongly (Sm1–O2 = 2.480(6) Å) than the THF molecule *trans* to the trimethylsilylmethyl group (Sm1–O1 = 2.588(6) Å). This difference can be rationalized either on the basis of steric repulsions between the apical THF ligand and the adjacent aryl substituents, or by the larger *trans* influence exerted by the alkyl ligand. The lengths of the phosphinimine P=N bonds (P1–N2 = 1.571(6) Å, P2–N3 = 1.593(6) Å) correlate well with other examples in the literature whereby the phosphinimine functionality exhibits considerable P=N double bond character.[49, 57, 67] Similar to other rare earth complexes supported by this ligand, the amido group of the pyrrole moiety is slightly closer (Sm1–N1 = 2.454(5) Å) to the metal centre than the phosphinimine nitrogen (Sm1–N3 = 2.582(6) Å), suggesting that the anionic charge is primarily localized on N1. Interestingly however, the other samarium–phosphinimine bond is significantly contracted (Sm–N2 = 2.436(6) Å), most likely due to the physical constraints imposed by the cyclometalation-induced metallacycle that encompasses the Pipp group of N1. Accordingly, the interatomic distance between the samarium centre and the *ortho*-carbon of the Pipp group indicates a Sm–C single bond (Sm1–C34 = 2.551(7) Å). Notably, the four-membered azasamaracycle is highly strained with bond angles deviating considerably from ideality (Sm1–C34–C29 = 93.5(5)º, C34–C29–N2 = 111.7(7)º, C29–N2–Sm1 = 98.2(4), N2–Sm1–C34 = 56.1(2)º).

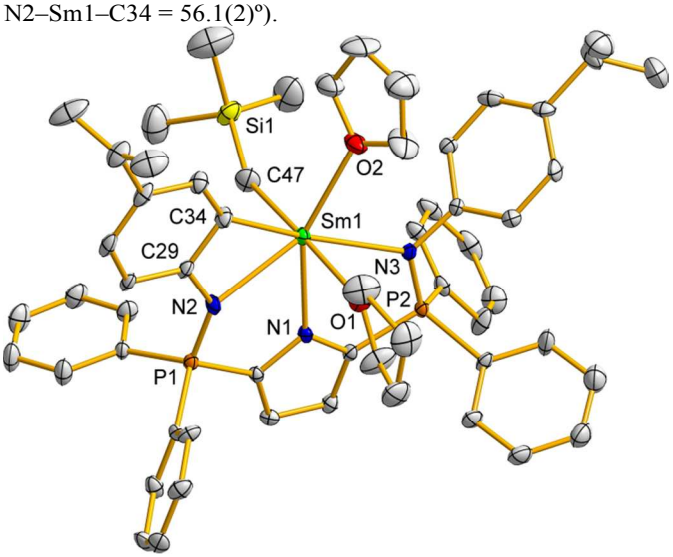

Figure 2 Thermal displacement plot (20% probability) of complex **2** with hydrogen atoms and minor disordered components omitted for clarity. Selected bond distances (Å) and angles (deg): P1−N2 = 1.571(6), P2−N3 = 1.593(6), Sm1–N1 = 2.454(5), Sm1–N2 = 2.436(6), Sm1–N3 = 2.582(6), Sm1–C34 = 2.551(7), Sm1–C47 = 2.470(10), Sm1–O1 = 2.588(6), Sm1–O2 = 2.480(6); C1–P1–N2 = 102.3(3), C4–P2—N3 = 105.6(3), C47–Sm1–O1 = 177.1(3), N1–Sm1–C34 = 159.4(2).

Although complex **2** is thermally stable in toluene solution at –35 ºC, it slowly converts into a different species at ambient temperature ($t_{½}$ = 1 h). This transformation is apparent when monitoring complex **2** by NMR spectroscopy, especially in the $^{31}P\{^{1}H\}$ spectra (benzene-d_6) wherein resonances at δ 24.5 and 18.1 from **2** are gradually replaced by two new signals at δ 39.4 and 24.7. As was discussed above for **2**, the two different phosphorus environments are indicative of ligand asymmetry. Moreover, the ^{1}H NMR spectrum exhibits resonances that suggest a species of increased complexity relative to that of **2**. In addition to an increase in aryl proton environments, the extrusion of one equivalent of tetramethylsilane was evident from the emergence of a singlet at δ 0.00. Owing to the proclivity of our carbazole-based bisphosphinimine complexes to undergo C–H activation at the *ortho*-position of the phosphorus phenyl substituents, we postulated this new compound might be the result of another ligand cyclometalation at the opposite phosphinimine P-aryl site (Scheme 3, **2a**), since a second N-Pipp activation would be expected to afford a symmetric species.

Through isolation of X-ray quality single crystals of this compound (*vide infra*), we were able to confirm that this complex was indeed the result of P-phenyl cyclometalation. However, the process appears to proceed at the phosphorus aryl group *adjacent* to the azasamaracycle and *inter*molecularly, ejecting an equivalent of TMS and forging several *C*- and *N*-bridging interactions to generate complex **3**, an unexpected *C*2-symmetric samarium dinuclear complex (Scheme 3, **3**). Spectroscopically, it would be difficult to distinguish between **2a** and **3**. As such, we were only able to ascertain the salient features of the structure of complex **3** from X-ray diffraction studies.

Similar to **2**, single crystals of **3** suitable for X-ray diffraction were grown by slow diffusion of pentane into a benzene solution of the complex at ambient temperature. The molecular structure of **3** is depicted in Figure 3 as a thermal displacement plot. Complex **3** features a samarium centre coordinated by one THF ligand, the three nitrogen atoms of the pyrrole bisphosphinimine scaffold, the carbon atom from the aforementioned azasamaracyle, one phosphinimine nitrogen atom from the opposing pyrrole ligand azasamaracycle, one of the *ortho* carbons from cyclometalation of the opposite pyrrole's azasamaracycle-adjacent phosphinimine phenyl groups, as well as the azasamaracyclic carbon from the opposite bisphosphinimine ligand. Considering these bonds are reciprocated at the other samarium atom, **3** involves pairs of μ-(phenylido)1κ*C*,2κ*C*, μ-(phosphinimine)1κ*N*,2κ*N*, and μ-(phosphiniminephenylido)1κ*N*,2κ*o*-*C* bridging groups. This represents a rare example of a dinuclear samarium complex possessing a bridging carbon atom, with only a few other dinuclear[68-72] or trinuclear[73, 74] complexes known. The bridging nature of these groups is evident from the close contacts (Sm1–C39 = 2.638(2), Sm1–N3 = 2.616(2), Sm1–C27 = 2.597(2) Å). As before, the azasamaracycle adopts a highly-strained 4-membered geometry (N3–Sm1–C39 = 52.54(5), Sm1–C39–C38 = 87.9(1), C39–C38–N3 = 108.7(2), C38–N3–Sm1 = 92.4(1)º).

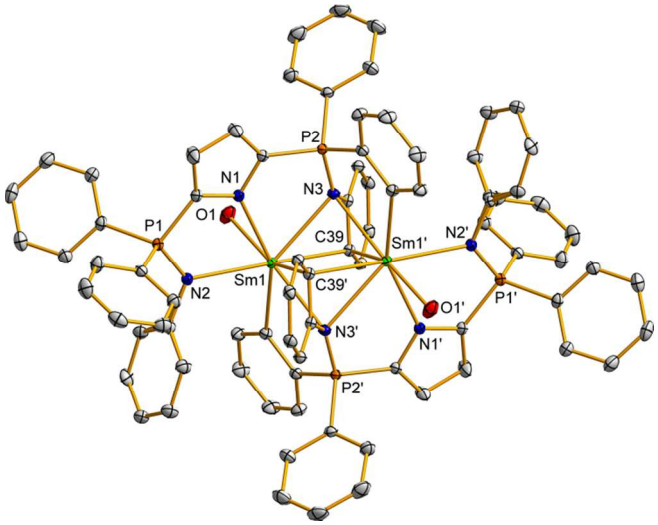

Figure 3 Thermal displacement plot (30% probability) of complex **3** with hydrogen atoms, benzene solvent molecules, THF backbones, Pipp ^{i}Pr groups, and minor disordered components omitted for clarity. Selected bond distances (Å) and angles (deg): P1−N2 = 1.600(2), P2−N3 = 1.609(1), Sm1–N1 = 2.477(2), Sm1–N2 = 2.530(2), Sm1–N3 = 2.616(2), Sm1–C39 = 2.638(2), Sm1–C27 = 2.597(2), Sm1–O1 = 2.575(2), Sm1···Sm1′ = 3.3655(6); P2–N3–C38 = 136.7(1), N3–P2–C26 = 109.0(1).

At 3.3655(6) Å, the distance between the samarium centres is too large to suggest Sm–Sm bonding. However, the interatomic distance is one of the shortest known, with reports by Gordon[75] and Gambarotta[76] being only marginally shorter, wherein they report distances of 3.3611(10) Å for [(μ-NC$_6$H$_3$^{i}Pr$_2$-2,6)Sm(μ-NHC$_6$H$_3$^{i}Pr$_2$-2,6)(μ-Me)AlMe$_2$]$_2$ and 3.4300(4) Å for [(Et$_8$-calix-pyrrole)Sm$_2$(THF)$_2$(μ-Cl)$_2$][Li(THF)$_2$], respectively. Although the shortest known Sm–Sm contact comes from a different report by Gambarotta (3.3159(5) Å) for [(OEPG)Sm$_2$(Et$_2$O)$_2$] (OEPG = deprotonated octaethylporphyrinogen), each samarium atom in that complex is formally described as Sm(II), and as a result, is likely involved in some degree of metal-metal bonding.[77]

The dinuclear nature of **3** represents the first example of a dinuclear samarium complex bridged by an η^1:μ^2-phenyl group and only the third example of the whole lanthanide series with a similar bridging fragment.[78, 79] Although the NMR spectral parameters of **3** indicate this complex is not strongly paramagnetic, analysis of this complex by air-sensitive SQUID measurements to determine its magnetic properties is still of interest, and the potential of the bridging system to evoke magnetic exchange coupling between samarium centres will be undertaken in due course.

As noted above, a variety of difficulties were encountered during the attempted preparation of complex **2'**. It was not until *slow*, dropwise addition of the proteo ligand H**L$_B$** into a solution of [Sm(CH$_2$SiMe$_3$)$_3$(THF)$_3$] was undertaken at low temperature that we were able to isolate a discrete complex (**2**). In an effort to establish possible competing reactions, we purposely added a solution of H**L$_B$** *rapidly* to a cooled (–35 ºC) toluene solution of [Sm(CH$_2$SiMe$_3$)$_3$(THF)$_3$]. Hence, we were able to identify complex **4** (Scheme 3) as the main product under such conditions. This doubly-ligated complex (*vide infra*) possesses *two* bisphosphinimine ligands, one of which contains the azasamaracyclic moiety in **2**. The two ancillary ligands are attached to Sm in an orthogonal arrangement that appears to leave insufficient space for Lewis basic solvent molecules to coordinate. Considering the structure of **4**, it is reasonable to postulate that **2** is an intermediate en route to complex **4**. To support this hypothesis, a sample of **2** was treated with excess H**L$_B$**, which resulted in formation of bis(ligated) complex **4**, as well as several other minor products.

The formulation of complex **4** was supported by spectroscopic analysis. Three signals are evident in the ^{31}P{^{1}H} NMR spectrum in a 1:1:2 ratio. The ligand asymmetry can also be seen in the ^{1}H NMR spectrum, whereby another complicated array of overlapping resonances is observed. Similar to complex **2**, four separate ^{i}Pr methyl and three separate ^{i}Pr methine signals were observed, but unlike either **2** or **3**, no THF resonances were visible.

The molecular structure of **4** is depicted in Figure 4 as a thermal displacement plot. As mentioned previously, complex **4** bears two inequivalent bisphosphinimine ligands, one with the κ^4 arrangement observed in complex **2** and one that is bound in a prototypical tridentate fashion. This base-free pseudopentagonal bipyramidal complex bears a strained metallacycle (Sm1–C34–C29 = 94.3(2)º, C34–C29–N2 = 111.6(3)º, C29–N2–Sm1 = 99.3(2)º, N2–Sm1–C34 = 54.8(1)º) and typical phosphinimine P=N (P1–N2 = 1.577(3) Å, P2–N3 = 1.597(3) Å), samarium-nitrogen (Sm1–N1 = 2.509(3) Å), and samarium-carbon bond lengths (Sm1–C34 = 2.603(4) Å). Notably, the angle at samarium involving the apical phosphinimine nitrogens (N12–Sm1–N13 = 136.21(9)º) is dramatically smaller than the corresponding angle in complex **2** (C47–Sm1–O1 = 177.1(3)º), presumably because N12 and N13 belong to the same pincer ligand.

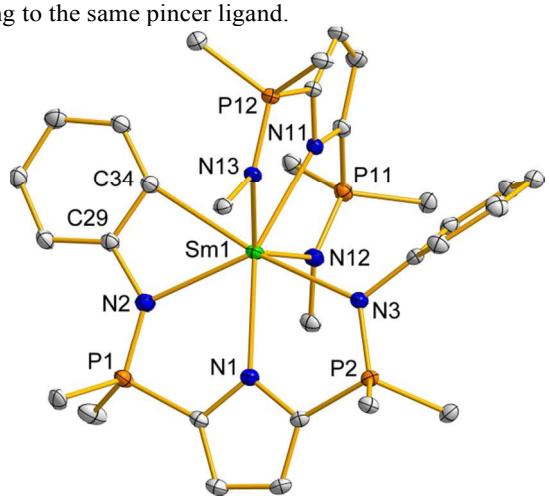

Figure 4. Thermal displacement plot (30% probability) of complex **4** with hydrogen atoms, P-phenyl rings (except *ipso* carbons), N-aryl rings (except *ipso* carbons) on the non-cyclometalated ligand and isopropyl substituents on the cyclometalated ligand omitted for clarity. Selected bond distances (Å) and angles (deg): P1–N2 = 1.577(3), P2–N3 = 1.597(3), Sm1–N11 = 2.509(3), Sm1–N2 = 2.471(3), Sm1–N3 = 2.615(3), Sm1–C34 = 2.603(4), Sm1–N11 = 2.466(2), Sm1–N12 = 2.469(2), Sm1–N13 = 2.472(3); N12–Sm1–N13 = 136.21(9).

Intriguingly, complex **4** bears a striking similarity to the cationic lutetium complex [(**L$_B$**)$_2$Lu]$^+$[B(C$_6$F$_5$)$_4$]$^-$ (**5**), which was produced as a disproportionation byproduct during the decomposition of previously reported [(**L$_B$**)Lu(CH$_2$SiMe$_3$)(OEt$_2$)$_2$]$^+$[B(C$_6$F$_5$)$_4$]$^-$ (**5'**).[57] Although only a small quantity of crystalline **5** was isolated, rendering further characterization impossible, it nonetheless serves as a useful crystallographic comparison to complex **4**. Both complexes feature two **L$_B$** derived ligands; however, the lutetium centre in

complex **5** exhibits a distorted octahedral geometry resulting from two tridentate $\mathbf{L_B}$ moieties (Figure 5). Furthermore, although the *trans* amido groups form an angle with Lu that is relatively close to 180º (N1–Lu1–N11 = 178.22(7)º), the other angles about the metal centre are severely strained (N2–Lu1–N3 = 143.90(7)º, N12–Lu1–N13 = 143.60(7)º). Also of interest is the fact that the lutetium amido bonds (Lu1–N1 = 2.340(2), Lu–N11 = 2.338(2) Å) are longer than the other lutetium-nitrogen distances (Lu–N2 = 2.324(2), Lu–N3 = 2.326(2), Lu–N12 = 2.326(2), Lu–N13 = 2.352(2) Å). This is most likely an artifact of the *trans* influence of these groups, which are located perfectly opposite to each other, unlike the other "*trans*" groups in this species.

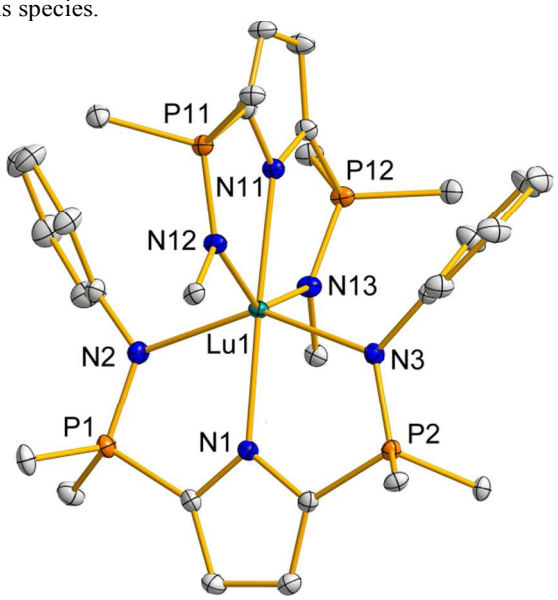

Figure 5. Thermal displacement plot (30% probability) of the cation of complex **5** with hydrogen atoms, non-*ipso* carbons of the P-phenyl rings, non-*ipso* carbons of the N12 and N13 N-aryl rings, isopropyl groups of the N3 and N3 N-aryl rings and minor disordered components omitted for clarity. Selected bond distances (Å) and angles (deg): P1−N2 = 1.634(2), P2−N3 = 1.637(2), P11−N12 = 1.642(2), P12−N13 = 1.637(2), Lu1–N1 = 2.340(2), Lu1–N2 = 2.324(2), Lu1–N3 = 2.326(2), Lu1–N11 = 2.338(2), Lu1–N12 = 2.326(2), Lu1–N13 = 2.352(2); N1–Lu1–N11 = 178.22(7), N2–Lu1—N3 = 143.90(7), N12–Lu1–N13 = 143.60(7).

Conclusions

Our newly reported pyrrole-based bisphosphinimine pincer ligand is able to support rare earth complexes of Y and Sm. In the case of Y, the ligated complex is resistant to cyclometalation, unlike its carbazole congener, and is notably free of Lewis bases, a testament to the versatility of this pyrrole system. Owing to the remarkable stability of these complexes, we are in the process of using this backbone to prepare mixed alkyl/amido yttrium complexes, which have the potential to lead to elusive rare earth imido complexes. Investigations in this area are on-going.

In the case of the larger, more reactive Sm, reaction of $[Sm(CH_2SiMe_3)_3(THF)_3]$ with $H\mathbf{L_B}$ is extremely facile, however the putative dialkyl complex $[\mathbf{L_B}Sm(CH_2SiMe_3)_2]$ immediately undergoes cyclometalation of an *N*-aryl group to form a somewhat "protected" variant $[\kappa^4$-$\mathbf{L_B}Sm(CH_2SiMe_3)(THF)_2]$ (**2**). This azasamaracyclic THF adduct is reasonably stable at low temperature and in the solid state, but it converts over time in solution to a unique carbon- and nitrogen-bridged dinuclear product $[\kappa^1{:}\kappa^2{:}\mu^2$-$\mathbf{L_B}Sm(THF)]_2$. However, if intercepted by another equivalent of $H\mathbf{L_B}$, the alkyl group of **2** appears to facilitate another alkane elimination reaction, resulting in a doubly-ligated samarium complex $[(\kappa^4$-$\mathbf{L_B})\mathbf{L_B}Sm]$ (**4**).

In many previous studies, dialkyl rare earth complexes have often been used to form alkyl/amido complexes $[L_nMR(NHR)]$ *via* the elimination of an alkyl group when a primary amine is added. These hybrid alkyl/amido species are of interest because a subsequent intramolecular alkane elimination reaction could potentially afford elusive rare earth imido $[L_nM{=}NR]$ complexes, which have been popularized in contemporary reports.[80, 81] Due to the presence of only one remaining $-CH_2SiMe_3$ group complex **2** cannot be used as a direct precursor to an alkyl/amido complex., Nonetheless, we were interested in preparing samarium amido complexes of the type $[\kappa^4$-$\mathbf{L_B}Sm(NHR)(THF)_x]$ as such complexes could potentially be transformed into terminal imido complexes if metallacycle ring-opening could be triggered intramolecularly,[50, 82] potentially forming a "decyclometalated" complex of the form $[\mathbf{L_B}Sm{=}NR(THF)_x]$. Unfortunately, complex **2** (as well as species **3** and **4**) did not react cleanly with a variety of different 1º amines, perhaps due to the exotic nature of the cyclometalated moiety. Regardless, we intend to further pursue amido and imido studies in due course. Finally, dinuclear product **4** has interesting potential from a single-molecule magnet (SMM) perspective, and studies in this area are ongoing, with intentions to expand this work to more prominent SMM metals such as dysprosium.

Experimental

Reagents and general procedures

Manipulations of air- and moisture-sensitive materials and reagents were carried out under an argon atmosphere using double vacuum manifold techniques or in a glove box. Solvents used for air- sensitive materials were purified using an MBraun solvent purification system (SPS), stored in PTFE-sealed glass vessels over sodium benzophenone ketyl (THF and ether) or "titanocene" (pentane, benzene, and toluene), and freshly distilled at the time of use. The deuterated solvents benzene-d_6 and toluene-d_8 were dried over sodium benzophenone ketyl, degassed *via* three freeze–pump–thaw cycles, distilled *in vacuo* and stored over 4 Å molecular sieves in glass bombs under argon. All NMR spectra were recorded at ambient temperature with a Bruker Avance II NMR spectrometer (300.13 MHz for ^{1}H, 75.47 MHz for ^{13}C, and 121.48 MHz for ^{31}P). Chemical shifts are reported in parts per million relative to the external standards $SiMe_4$ (^{1}H, ^{13}C) and 85% H_3PO_4 (^{31}P); residual H-containing species in benzene-d_6 (δ 7.16) were used as internal references (^{1}H). Assignments were aided by the use of $^{13}C\{^1H\}$-DEPT and ^1H–$^{13}C\{^1H\}$-HSQC experiments (s = singlet, d = doublet, t = triplet, q = quartet, sp = septet, m = multiplet, br = broad, ov = overlapping signals). Elemental analyses were performed using an Elementar Vario Microcube instrument.[83] The reagents $[YCl_3(THF)_3]$, $[Y(CH_2SiMe_3)_3(THF)_2]$, *N*,*N*'-((1*H*-pyrrole-2,5-diyl)bis(diphenylphosphoranylylidene))bis(4-*iso*propylaniline) ($H\mathbf{L_B}$),[57] $[Sm(CH_2SiMe_3)_3(THF)_3]$,[65] and $[(\mathbf{L_B})Lu(CH_2SiMe_3)(OEt_2)_2]^+[B(C_6F_5)_4]^-$ (**5'**)[57] were prepared

Table 1. Summary of X-ray crystallography data collection and structure refinement for compounds **1**, **2**, **3** · 2 benzene, **4**, and **5**

	1	**2**	**3** · 2 C_6H_6	**4**	**5**
Formula	$C_{54}H_{66}N_3P_2SiY$	$C_{58}H_{70}N_3O_2P_2SiSm$	$C_{100}H_{100}N_6O_2P_4Sm_2 \cdot 2\ C_6H_6$	$C_{92}H_{87}N_6P_4Sm$	$C_{116}H_{88}BF_{20}\ LuN_6P_4$
Formula weight (g mol^{-1})	964.12	1081.55	1998.65	1550.90	2255.58
Crystal system	Triclinic	Monoclinic	Monoclinic	Triclinic	Orthorhombic
Space group	*P*–1	$P2_1/c$	$P2_1/n$	*P*–1	*Pbca*
Unit cell parameters					
a (Å)	9.7370(7)	14.806(2)	15.9755(13)	12.3595(11)	21.649(5)
b (Å)	12.1842(9)	14.713(2)	17.8486(15)	13.8452(12)	22.032(5)
c (Å)	24.1371(18)	29.208(5)	17.3855(14)	24.642(2)	45.231(10)
α (°)	84.8276(9)	90	90	104.3038(9)	90
β (°)	78.9662(9)	101.263(2)	109.2030(10)	101.2213(9)	90
γ (°)	69.6098(9)	90	90	95.5028(9)	90
V ($Å^3$)	2633.7(3)	6240.0(18)	4681.5(7)	3961.6(6)	21574(8)
Z	2	4	2	2	8
ρ_{calcd} (mg m^{-3})	1.216	1.151	1.418	1.300	1.389
μ (mm^{-1})	1.250	1.049	1.366	0.872	1.060
Crystal dimensions (mm)	0.30 × 0.16 × 0.16	0.43 × 0.33 × 0.30	0.31 × 0.17 × 0.11	0.30 × 0.24 × 0.16	0.36 × 0.15 × 0.15
Crystal colour	Colourless	Yellow	Yellow	Light red	Colourless
Crystal habit	Needle	Block	Prism	Block	Prism
θ range (°)	1.72 to 25.00	1.56 to 25.00	1.69 to 26.00	0.875 to 25.00	1.597 to 26.00
Diffractometer	Bruker D8/APEX II CCD[i]				
Radiation (λ[Å])	Mo Kα (0.71073) fine focused sealed tube source				
Temperature (K)	173	173	173	173	173
Total data collected	25832	72436	48294	56897	295374
Independ reflns (R_{int})	9252 (0.0208)	10985 (0.0434)	8272 (0.0219)	13911(0.0905)	21194(0.0524)
Obsd reflns [$F_o^2 \geq 2\sigma(F_o^2)$]	8315	9375	9183	11555	17241
Restraints/params	142 / 590	237 / 719	48 / 587	66 / 993	51 / 1371
Goodness-of-fit (*S*)[ii] [all data]	1.136	1.202	1.061	1.044	1.080
Final *R* indices[iii]					
R_1 [$F_o^2 \geq 2\sigma(F_o^2)$]	0.0403	0.0788	0.0199	0.0384	0.0285
wR_2 [$F_o^2 \geq 2\sigma(F_o^2)$]	0.0999	0.1761	0.0473	0.0931	0.0646
R_1 [all data]	0.0460	0.0899	0.0244	0.0487	0.0406
wR_2 [all data]	0.1031	0.1798	0.0499	0.0965	0.0686
Largest diff peak, hole (e $Å^{-3}$)	0.786 and –0.513	1.431 and –3.086	0.549 and –0.305	1.579 and –0.581	0.428 and –0.380

[i] Programs for diffractometer operation, data collection, data reduction, and absorption correction were those supplied by Bruker.
[ii] $S = [w(F_o^2 - F_c^2)^2/(n-p)]^{1/2}$ (*n* = number of data; *p* = number of parameters varied; $w = [\sigma^2(F_o^2) + (0.0540P)^2 + 22.8160P]^{-1}$ where $P = [\mathrm{Max}(F_o^2, 0) + 2F_c^2]/3$).
[iii] $R_1 = \Sigma||F_o| - |F_c||/\Sigma|F_o|$; $wR_2 = [\Sigma w(F_o^2 - F_c^2)^2/\Sigma w(F_o^4)]^{1/2}$.

according to literature methods. Complex **5** was isolated as a minor disproportionation byproduct from decomposition of **5'** in benzene over several days. Although reported previously by other methods,[84, 85] $[SmCl_3(THF)_2]$ was prepared in our laboratory from a modified procedure as described below. A solid sample of $LiCH_2SiMe_3$ was obtained by removal of pentane from a 1.0 M solution purchased from Sigma-Aldrich. A sample of 6.0 M HCl was prepared by dilution of a concentrated solution. All other reagents were purchased from commercial sources and used as received.

Synthesis of Compounds

$[SmCl_3(THF)_2]$. This complex was prepared *via* a modified literature procedure.[84, 85] A sample of $[Sm_2O_3]$ (5.211g, 14.94 mmol) was added to a 250 mL round-bottomed flask and dissolved in 6.0 M HCl (30 mL). The flask was attached to a reflux condensor, and the solution was heated at reflux for 23 h. The volatiles were then removed *in vacuo* to afford $[SmCl_3(H_2O)_6]$ as a yellow residue. A solution of $SOCl_2$ (35 mL, 0.48 mol) in THF (90 mL) was slowly added to the residue. After bubbling had subsided, the solution was heated at reflux for 14 h, at which point volatiles were removed *in vacuo* resulting in a pale yellow solid. The flask was connected to a swivel frit apparatus which was then attached to a double vacuum manifold. A portion of Et_2O (70 mL) was transferred to the flask, the slurry was vigorously mixed, then filtered and the resulting white powder was dried *in vacuo* (10.784 g, 90%). ^1H NMR (benzene-d_6): δ 3.58 (m, 8H, THF OCH_2); 1.41 (m, 8H, THF OCH_2CH_2). Accurate $^{13}C\{^1H\}$ NMR spectral data could not be obtained because of insolubility of $[SmCl_3(THF)_2]$ in common organic solvents. Anal. Calcd. (%) for $C_8H_{16}Cl_3O_2Sm$: C, 23.97; H, 4.02. Found: C, 23.48; H, 3.71.

$[L_BY(CH_2SiMe_3)_2]$ (1). In an argon atmosphere glove box, anhydrous yttrium chloride (168 mg, 0.86 mmol) was weighed into a 50 mL 2-neck round-bottomed flask and 4 mL of a THF/pentane mixture (3:1) was added to form an off-white slurry. The flask was connected to a swivel frit apparatus, attached to a double vacuum manifold, and heated at 65 ºC for 1.5 h. In a separate 50 mL 2-neck flask, $LiCH_2SiMe_3$ (246 mg, 2.61 mmol) was dissolved in 4 mL of a THF/pentane mixture (1:3) and the resulting suspension was added to the other flask dropwise over 5 min at –94 ºC *via* cannula. The mixture was allowed to warm to 0 ºC and stirred for an additional 3.5 h at that temperature. The THF/pentane solution was removed *in vacuo* to yield a white solid. In an argon atmosphere glove box, proteo ligand HL_B (595 mg, 0.85 mmol) was added to a different 50 mL two-neck round-bottom flask, dissolved in 15 mL of toluene and attached to a double vacuum manifold. The proteo ligand solution was added dropwise over 5 min to the reaction mixture *via* cannula, and the solution was stirred at ambient temperature for 1 h. The resulting cloudy yellow solution was filtered and the solid was washed three times with 10 mL pentane. All solvents were evaporated under reduced

pressure yielding an oily yellow solid. The solid was then triturated once with 25 mL of pentane and dried *in vacuo* to yield a light yellow powder (616 mg, 75%). ^{1}H NMR (benzene-d_6): δ 7.71 (ddd, $^3J_{H–P}$ = 12.3 Hz, $^3J_{H–H}$ = 7.8 Hz, $^4J_{H–H}$ = 1.2 Hz, 8H, *o*-phenyl *H*); 7.38 (dd, $^3J_{H–H}$ = 8.5 Hz, $^4J_{H–P}$ = 2.1 Hz, 4H, *o*-Pipp *H*); 7.06 (d, $^3J_{H–H}$ = 8.1 Hz, 4H, *m*-Pipp *H*); 7.07–6.90 (ov m, 12H, *m*-phenyl + *p*-phenyl *H*); 6.63 (dd, $^3J_{H–P}$ = 2.1 Hz, $^4J_{H–P}$ = 1.2 Hz, 2H, pyrrole C*H*); 2.66 (sp, $^3J_{H–H}$ = 6.6 Hz, 2H, ^{i}Pr C*H*); 1.10 (d, $^3J_{H–H}$ = 7.0 Hz, 12H, ^{i}Pr CH_3); 0.21 (s, 18H, YCH$_2$Si(CH_3)$_3$), −0.04 (d, $^2J_{H–Y}$ = 2.8 Hz, 4H, YCH_2). ^{13}C{^{1}H} NMR (benzene-d_6): δ 144.3 (m, 2C), 143.0 (d, 4C, $^1J_{C–P}$ = 6.0 Hz, aromatic *ipso*-*C*); 133.6 (d, 8C, $^3J_{C–P}$ = 10.4 Hz), 132.7 (s, 4C, aromatic *C*H); 131.7 (s, 2C, aromatic *C*); 130.5 (s, 2C, aromatic *ipso*-*C*); 129.1 (d, 8C, $^2J_{C–P}$ = 12.7 Hz), 128.4 (d, 4C, $^4J_{C–P}$ = 8.2 Hz), 128.1 (s, 4C, aromatic *C*H); 119.4 (dd, 2C, $^2J_{C–P}$ = 28.0 Hz, $^3J_{C–P}$ = 6.0 Hz, pyrrole *C*H); 34.5 (d, 2C, $^1J_{C–Y}$ = 39 Hz, Y*C*H$_2$); 34.2, (s, 2C, ^{i}Pr *C*H), 24.6 (s, 4C, ^{i}Pr *C*H$_3$), 5.1 (s, 6C, Si(*C*H$_3$)$_3$). ^{31}P{^{1}H} NMR (benzene-d_6): δ 25.0 (d, $^3J_{P–Y}$ = 7.5 Hz). Anal. Calcd. (%) for $C_{54}H_{66}N_3P_2Si_2Y$: C, 67.27; H, 6.90; N, 4.36. Found: C, 66.90; H, 6.51; N, 4.53.

[κ^4-L$_B$Sm(CH$_2$SiMe$_3$)(THF)$_2$] (2). In an argon atmosphere glove box, [SmCl$_3$(THF)$_2$] (230 mg, 0.57 mmol) was weighed into a 50 mL 2-neck round-bottomed flask. A THF/pentane mixture (3:1, 6 mL) was added to form an off-white slurry. The flask was connected to a swivel frit apparatus which was then attached to a double vacuum manifold. In a separate 50 mL 2-neck flask, LiCH$_2$SiMe$_3$ (162 mg, 1.72 mmol) was dissolved in 6 mL of a THF/pentane mixture (1:3) and cooled to 0 ºC. After 5 min, the resulting suspension of LiCH$_2$SiMe$_3$ was added to the other flask dropwise over 1 min at –78 ºC *via* cannula. The mixture was stirred for an additional 3 h at that temperature, wherein the solution turned bright yellow in colour. The THF/pentane solution was removed *in vacuo* at –35 ºC to afford a yellow solid, at which point a portion of toluene (5 mL) was added. In an argon atmosphere glove box, proteo ligand H**L$_B$** (410 mg, 0.58 mmol) was added to a separate 50 mL two-neck round-bottom flask, dissolved in 9 mL of toluene and attached to a double vacuum manifold. The proteo ligand solution was added dropwise to the reaction mixture over 1 min at –78 ºC *via* cannula, and the resulting solution was allowed to gradually warm to ambient temperature whereupon it was stirred for 1 h. The resulting orange solution was filtered and the solvent was removed under reduced pressure. The resulting orange solid was triturated with pentane and dried *in vacuo*. The residue was recrystallized from a concentrated solution of THF (2 mL) layered with pentane (15 mL), washed with 5 × 2 mL pentane, and dried *in vacuo* to yield a dark orange powder (444 mg, 72%). ^{1}H NMR (benzene-d_6): δ 9.42 (m, 2H), 9.21 (m, 2H), 8.29 (m, 1H), 8.08 (m, 1H), 7.77 (m, 2H), 7.48 (m, 7H), 7.05 (m, 4H), 6.87 (m, 4H), 6.61 (m, 4H, Ar); 5.34 (m, 2H, pyrrole C*H*); 3.17 (br s, 8H, THF OCH_2); 1.63 (d, $^3J_{H–H}$ = 7.2 Hz, 3H), 1.59 (d, $^3J_{H–H}$ = 6.9 Hz, 3H, ^{i}Pr CH_3); 1.30 (ov, 1H, ^{i}Pr C*H*); 1.21 (br m, 8H, THF OCH$_2$CH_2); 1.08 (ov, 1H, ^{i}Pr CH); 0.89 (s, 2H, SmCH_2); –0.14 (d, $^3J_{H–H}$ = 5.7 Hz, 3H), –0.54 (d, $^3J_{H–H}$ = 6.6 Hz, 3H, ^{i}Pr CH_3); –3.75 (s, 9H, SmCH$_2$Si(CH_3)$_3$). Accurate ^{13}C{^{1}H} NMR spectral data could not be obtained because of rapid decomposition of the sample to **3** in solution. Low temperature studies were attempted in an effort to slow this decomposition process, but signals became sufficiently broad that signal-to-noise ratios were unsatisfactory. ^{31}P{^{1}H} NMR (benzene-d_6): δ 24.5 (s), 18.1 (s). Anal. Calcd. (%) for $C_{58}H_{70}N_3O_2P_2SiSm_2$: C, 64.41; H, 6.52; N, 3.89. Found: C, 64.77; H, 6.71; N, 4.05.

[κ^1:κ^2:μ^2-L$_B$Sm(THF)]$_2$ (3). In an argon atmosphere glove box, [κ^4-**L$_B$**Sm(CH$_2$SiMe$_3$)(THF)$_2$] (243 mg, 0.22 mmol) was weighed into a 50 mL round-bottomed flask and 9 mL of toluene was added to form an orange slurry. The flask was attached to a double vacuum manifold and warmed to 50 ºC for 3 h. The solution was then cooled to ambient temperature and all volatiles were removed *in vacuo*. The solid was recrystallized from a concentrated solution of benzene (7 mL) layered with pentane (20 mL), collected by filtration, washed with 5 × 2 mL pentane, and dried under vacuum to yield a dark orange powder. The solid was redissolved in toluene (15 mL), and the solution stored at –35 ºC for 12 h. The resulting precipitate was collected by filtration, washed with pentane, and dried *in vacuo* yielding a dark orange solid (207 mg, 51%). ^{1}H NMR (benzene-d_6): δ 10.61 (m, 2H), 10.16 (m, 2H), 9.13 (m, 2H), 8.92 (m, 2H), 8.80 (m, 2H), 8.64 (m, 6H), 8.50 (m, 4H), 8.38 (m, 2H), 8.15 (m, 2H), 7.00 (m, 16H), 6.63 (m, 6H), 6.47 (m, 6H, Ar); 6.19 (m, 4H, pyrrole C*H*); 3.35 (m, 8H, THF OCH_2); 2.49 (sp, $^3J_{H–H}$ = 7.3 Hz, 2H), 1.34 (sp, $^3J_{H–H}$ = 6.9 Hz, 2H, ^{i}Pr C*H*); 1.13 (d, $^3J_{H–H}$ = 6.9 Hz, 6H), 1.09 (d, $^3J_{H–H}$ = 6.9 Hz, 6H), 0.49 (d, $^3J_{H–H}$ = 6.9 Hz, 6H), –0.21 (d, $^3J_{H–H}$ = 8.4 Hz, 6H, ^{i}Pr CH_3); –0.51 (br s, 8H, THF OCH$_2$CH_2). ^{13}C{^{1}H} NMR (benzene-d_6): δ 146.9 (s, 2C), 146.8 (s, 2C), 141.2 (s, 2C), 141.1 (s, 2C), 138.2 (s, 2C, Pipp *C*); 136.8 (d, 2C, $^2J_{C–P}$ = 6.6 Hz, aromatic *C*); 136.7 (s, 2C, aromatic *C*H); 135.5 (d, 2C, $^1J_{C–P}$ = 71.5 Hz, pyrrole *C*); 135.3 (d, 4C, $^1J_{C–P}$ = 10.0 Hz, aromatic *ipso*-*C*); 134.3 (d, 8C, $^2J_{C–P}$ = 9.0 Hz), 133.9 (d, 8C, $^2J_{C–P}$ = 10.0 Hz, aromatic *C*H); 131.8 (d, 2C, $^1J_{C–P}$ = 88.6 Hz, pyrrole *C*); 131.8 (d, 4C, $^2J_{C–P}$ = 9.4 Hz), 131.8 (d, 4C, $^3J_{C–P}$ = 5.5 Hz), 131.3 (s, 4C), 131.2 (s, 2C, aromatic *C*H); 129.7 (om m, 2C, pyrrole *C*H); 129.7 (s, 4C, aromatic *C*H); 129.3 (d, 2C, $^1J_{C–P}$ = 24.2 Hz, aromatic *ipso*-*C*); 129.2 (s, 2C, pyrrole *C*H); 127.5 (s, 4C, aromatic *C*H); 126.9 (d, 2C, $^1J_{C–P}$ = 7.0 Hz, aromatic *ipso*-*C*); 126.3 (br s, 2C), 126.0 (s, 2C), 123.3 (s, 2C), 123.3 (s, 2C), 121.7 (s, 4C, aromatic *C*H); 105.8 (br s, 4C, THF O*C*H$_2$); 34.2 (s, 2C), 31.5 (s, 2C, ^{i}Pr *C*H); 24.8 (s, 2C), 24.5 (s, 2C), 24.2 (s, 2C), 24.0 (s, 2C, ^{i}Pr *C*H$_3$); 21.8 (s, 4C, THF OCH$_2$*C*H$_2$). ^{31}P{^{1}H} NMR (benzene-d_6): δ 39.4 (s), 24.7 (s). Anal. Calcd. (%) for $C_{100}H_{100}N_6O_2P_4Sm_2$: C, 65.19; H, 5.47; N, 4.56. Found: C, 66.07; H, 5.62; N, 4.39.

[(κ^4-L$_B$)L$_B$Sm] (4). In an argon atmosphere glove box, [SmCl$_3$(THF)$_2$] (357 mg, 0.89 mmol) was weighed into a 50 mL 2-neck round-bottomed flask and 6 mL of a THF/pentane mixture (3:1) was added to form an off-white slurry. The flask was connected to a swivel frit apparatus which was then attached to a double vacuum manifold. In a separate 50 mL 2-neck flask, LiCH$_2$SiMe$_3$ (252 mg, 2.68 mmol) was dissolved in 6 mL of a THF/pentane mixture (1:3) and cooled to 0 ºC. After 5 min, the resulting suspension of LiCH$_2$SiMe$_3$ was quickly added to the other flask dropwise over 1 min at –35 ºC *via* cannula. The mixture was stirred for an additional 3 h at that temperature, wherein the solution turned bright yellow in colour. The THF/pentane solution was removed *in vacuo* at –35 ºC to yield a yellow solid, at which point a portion of toluene (5 mL) was added. In an argon atmosphere glove box, proteo ligand H**L$_B$** (625 mg, 0.89 mmol) was added to a different 50 mL two-neck round-bottom flask, dissolved in 18 mL of toluene and attached to a double vacuum manifold. The proteo ligand solution was quickly added to the reaction mixture at –35 ºC *via* cannula, and the solution was allowed to warm to ambient temperature and stirred for an additional 1 h. The resulting orange solution was filtered using a swivel frit apparatus and the volatiles removed under vacuum. The orange solid was triturated 3 times with 3 mL of pentane and dried *in*

vacuo. The resulting residue was recrystallized from a concentrated solution of THF (5 mL) layered with pentane (20 mL), washed with 5 × 2 mL pentane, and dried under vacuum to yield a dark orange powder (622 mg, 45%). ^{1}H NMR (benzene-d_6): δ 10.52 (dd, 1H, $J_{H–P}$ = 11.1 Hz, $J_{H–H}$ = 7.8 Hz), 10.28 (dd, 2H, $J_{H–P}$ = 3.3 Hz, $J_{H–H}$ = 3.3 Hz), 9.28 (br s, 1H), 8.98 (m, 2H, $J_{H–H}$ = 3.3 Hz), 8.78 (dd, 1H, $J_{H–P}$ = 12.9 Hz, $J_{H–H}$ = 7.2 Hz), 8.55 (m, 4H), 8.21 (m, 6H), 8.09 (m, 1H, $J_{H–H}$ = 3.3 Hz), 8.00 (br s, 1H), 7.92 (br s, 1H), 7.23 (m, 4H, $J_{H–H}$ = 3.3 Hz), 6.89 (m, 19H), 6.36 (m, 6H), 6.68 (d, 4H, $J_{H–H}$ = 7.8 Hz, aromatic C*H*); 3.57 (sp, 1H, $J_{H–H}$ = 6.9 Hz), 2.93 (sp, 1H, $J_{H–H}$ = 6.9 Hz, ^{i}Pr C*H*); 1.95 (d, 6H, $J_{H–H}$ = 6.9 Hz, ^{i}Pr CH_3); 1.70 (sp, 2H, $J_{H–H}$ = 6.9 Hz, ^{i}Pr C*H*); 1.39 (d, 6H, $J_{H–H}$ = 6.9 Hz), 0.46 (d, 6H, $J_{H–H}$ = 6.9 Hz), 0.43 (d, 6H, $J_{H–H}$ = 6.9 Hz, ^{i}Pr CH_3). ^{13}C{^{1}H} NMR (benzene-d_6): δ 137.4 (s, 2C), 137.2 (s, 1C), 137.1 (m, 1C), 137.0 (m, 1C), 136.2 (s, 1C), 135.3 (d, 2C, $J_{C–P}$ = 9.0 Hz), 135.1 (d, 2C, $J_{C–P}$ = 8.5 Hz, aromatic *ipso*-*C*); 134.6 (dd, 8C, $J_{C–P}$ = 9.3 Hz, $J_{C–P}$ = 9.3 Hz), 133.9 (d, 4C, $J_{C–P}$ = 9.1 Hz), 133.8 (d, 8C, $J_{C–P}$ = 10.4 Hz), 133.4 (d, 4C, $J_{C–P}$ = 10.4 Hz, aromatic *C*H); 132.2 (s, 2C), 131.8 (m, 2C, aromatic *ipso*-*C*); 131.5 (ov m, 4C), 131.4 (ov m, 2C), 131.3 (ov m, 1C), 131.2 (ov m, 1C, aromatic *C*H); 130.5 (s, 1C), 129.8 (s, 1C), 129.2 (ov m, 4C, $J_{C–P}$ = 6.0 Hz, aromatic *ipso*-*C*); 127.5 (s, 4C), 127.3 (s, 4C), 127.1 (s, 2C), 127.0 (s, 2C), 126.4 (s, 1C, aromatic *C*H); 126.1 (1C, aromatic *ipso*-*C*); 124.7 (s, 8C), 123.9 (s, 1C), 121.9 (s, 1C), 118.1 (s, 2C), 118.0 (s, 2C, aromatic *C*H); 34.8 (s, 1C), 32.8 (s, 2C), 31.5 (s, 1C, ^{i}Pr *C*H); 26.3 (s, 2C), 25.0 (s, 2C), 24.1 (s, 2C); 23.1 (s, 2C, ^{i}Pr *C*H_3). ^{31}P{^{1}H} NMR (benzene-d_6): δ 40.8 (s, 1P), 26.3 (s, 1P), 19.3 (s, 2P). Anal. Calcd. (%) for $C_{92}H_{87}N_6P_4Sm$: C, 71.24; H, 5.65; N, 5.42. Found: C, 70.87; H, 6.05; N, 5.16.

X-ray crystallography

Single crystals suitable for X-ray diffraction were readily obtained from slow diffusion of pentane into a concentrated toluene (**1**) or THF solution (**2**) at –35 ºC, from slow diffusion of pentane into a concentrated benzene (**3**) or THF solution (**4**) at ambient temperature, or from slow evaporation of a concentrated benzene solution (**5**). Crystals were coated in dry Paratone oil under an argon atmosphere and mounted onto a glass fibre. Data were collected at 173 K using a Bruker SMART APEX II diffractometer (Mo Kα radiation, λ = 0.71073 Å) outfitted with a CCD area-detector and a KRYO-FLEX liquid nitrogen vapour cooling device. A data collection strategy using ω and φ scans at 0.5º steps yielded full hemispherical data with excellent intensity statistics. Unit cell parameters were determined and refined on all observed reflections using APEX2 software.[86] Data reduction and correction for Lorentz polarization were performed using SAINT-Plus software.[87] Absorption corrections were applied using SADABS.[88] The structures were solved by direct methods and refined by the least squares method on F^2 using the SHELXTL software suite.[89] All non-hydrogen atoms were refined anisotropically. Hydrogen atom positions were calculated and isotropically refined as riding models to their parent atoms. Table 1 provides a summary of selected data collection and refinement parameters.

Special considerations were required in the refinement of disordered moieties in all determined structures. One of the ^{i}Pr groups in **1** was found to be in two different orientations which were refined with occupation ratios of 61:39. For **2** and **3**, the whole non-cyclometalated Pipp phenyl ring was disordered in two positions which could be refined with approximate 57:43 and 56:44 occupancy ratios, respectively. Furthermore, the coordinated THF molecules of **2** were also disordered in two positions with an occupation ratio of 64:36. Finally, one ^{i}Pr carbon (C36) of the cyclometalated Pipp ring in **2** was disordered and refined in two positions (57:43). In **4**, both phenyl groups attached to phosphorus P1 were disordered over two positions and were refined to these positions with occupation ratios of 56:44 and 51:49. In addition, two of the ^{i}Pr groups were disordered in two positions and refined with the occupation ratio of 61:39 and 69:31. The disorder of one of the ^{i}Pr groups in **5** was refined with an occupation ratio of 76:24.

No suitable disorder model could be found for the severely disordered solvent molecules (THF or benzene) in **2**, **4** or **5**; hence, electron density associated with the solvent molecules was treated with the solvent mask option as implemented in the Olex2 program.[90]

Acknowledgments

This research was financially supported by the Natural Sciences and Engineering Research Council (NSERC) of Canada and the Canada Foundation for Innovation (CFI). Prof. Jun Okuda and RWTH Aachen University are thanked for hosting PGH during the preparation of this manuscript. Dr. Tracey Roemmele is acknowledged for aiding with elemental analysis measurements.

Notes

Department of Chemistry and Biochemistry, University of Lethbridge, 4401 University Drive, Lethbridge, AB, Canada, T1K 3M4

Electronic Supplementary Information (ESI) available: CCDC 991840 (**1**), 991841 (**2**), 991842 (**3**), 991843 (**4**), and 991844 (**5**). For atomic coordinates, interatomic distances, and angles, anisotropic thermal parameters, and hydrogen parameters for **1**, **2**, **3**, **4**, and **5** in a CIF file, see DOI: 10.1039/b000000x/.

References

1 S. Zhou, H. Wang, J. Ping, S. Wang, L. Zhang, X. Zhu, Y. Wei, F. Wang, Z. Feng, X. Gu, S. Yang, and H. Miao, *Organometallics*, 2012, **31**, 1696-1702.
2 G. Jeske, H. Lauke, H. Mauermann, H. Schumann, and T. J. Marks, *J. Am. Chem. Soc.*, 1985, **107**, 8111-8118.
3 G. A. Molander and J. O. Hoberg, *J. Org. Chem.*, 1992, **57**, 3266-3268.
4 G. A. Molander and J. A. C. Romero, *Chem. Rev.*, 2002, **102**, 2161-2185.
5 Y. Obora, T. Ohta, C. L. Stern, and T. J. Marks, *J. Am. Chem. Soc.*, 1997, **119**, 3745-3755.
6 M. A. Giardello, V. P. Conticello, L. Brard, M. R. Gagné, and T. J. Marks, *J. Am. Chem. Soc.*, 1994, **116**, 10241-10254.
7 T. Shima and Z. Hou, *J. Am. Chem. Soc.*, 2006, **128**, 8124-8125.
8 S. Hong and T. J. Marks, *Acc. Chem. Res.*, 2004, **37**, 673-686.
9 T. E. Müller, K. C. Hultzsch, M. Yus, F. Foubelo, and M. Tada, *Chem. Rev.*, 2008, **108**, 3795-3892.
10 G. A. Molander and E. D. Dowdy, *J. Org. Chem.*, 1998, **63**, 8983-8988.
11 V. M. Arredondo, F. E. McDonald, and T. J. Marks, *Organometallics*, 1999, **18**, 1949-1960.
12 J.-S. Ryu, G. Y. Li, and T. J. Marks, *J. Am. Chem. Soc.*, 125, **125**, 12584-12605.
13 A. Motta, I. L. Fragalà, and T. J. Marks, *Organometallics*, 2006, **25**, 5533-5539.
14 H. F. Yuen and T. J. Marks, *Organometallics*, 2009, **28**, 2423-2440.
15 A. G. Trambitas, T. K. Panda, J. Jenter, P. W. Roesky, C. Daniliuc, C. G. Hrib, P. G. Jones, and M. Tamm, *Inorg. Chem.*, 2010, **49**, 2435-2446.
16 D. V. Gribkov, F. Hampel, and K. C. Hultzsch, *Eur. J. Inorg. Chem.*, 2004, 4091-4101.
17 G. A. Molander and M. Julius, *J. Org. Chem.*, 1992, **57**, 6347-6351.
18 P.-F. Fu, L. Brard, Y. Li, and T. J. Marks, *J. Am. Chem. Soc.*, 1995, **117**, 7157-7168.

19 G. A. Molander and W. H. Retsch, *J. Am. Chem. Soc.*, 1997, **119**, 8817-8825.
20 G. A. Molander, E. D. Dowdy, and B. C. Noll, *Organometallics*, 1998, **17**, 3754-3758.
21 M. R. Douglass and T. J. Marks, *J. Am. Chem. Soc.*, 2000, **122**, 1824-1825.
22 M. R. Douglass, C. L. Stern, and T. J. Marks, *J. Am. Chem. Soc.*, 2001, **123**, 10221-10238.
23 A. M. Kawaoka, M. R. Douglass, and T. J. Marks, *Organometallics*, 2003, **22**, 4630-4632.
24 A. Motta, I. L. Fragalà, and T. J. Marks, *Organometallics*, 2005, **24**, 4995-5003.
25 K. N. Harrison and T. J. Marks, *J. Am. Chem. Soc.*, 1992, **114**, 9220-9221.
26 H. Schumann, A. Heim, J. Demtschuk, and S. H. Mühle, *Organometallics*, 2003, **22**, 118-128.
27 S. Seo, X. Yu, and T. J. Marks, *J. Am. Chem. Soc.*, 2009, **131**, 263-276.
28 X. Yu, S. Seo, and T. J. Marks, *J. Am. Chem. Soc.*, 2007, **129**, 7244-7245.
29 S. Seo and T. J. Marks, *Chem. Eur. J.*, 2010, **16**, 5148-5162.
30 A. Motta, I. L. Fragalà, and T. J. Marks, *Organometallics*, 2010, **29**, 2004-2012.
31 H. Schumann, J. A. Meese-Marktscheffel, and L. Esser, *Chem. Rev.*, 1995, **95**, 865-986.
32 S. Zhou, S. Wu, H. Zhu, S. Wang, X. Zhu, L. Zhang, G. Yang, D. Cui, and H. Wang, *Dalton Trans.*, 2011, **40**, 9447-9453.
33 P. L. Watson and G. W. Parshall, *Acc. Chem. Res.*, 1985, **18**, 51-56.
34 G. Jeske, H. Lauke, H. Mauermann, P. N. Swepston, H. Schumann, and T. J. Marks, *J. Am. Chem. Soc.*, 1985, **107**, 8091-8103.
35 W. J. Evans, T. A. Ulibarri, and J. W. Ziller, *J. Am. Chem. Soc.*, 1990, **112**, 2314.
36 M. A. Giardello, Y. Yamamoto, L. Brard, and T. J. Marks, *J. Am. Chem. Soc.*, 1995, **117**, 3276-3277.
37 M. Yamashita, Y. Takemoto, E. Ihara, and H. Yasuda, *Macromolecules*, 1996, **29**, 1798-1806.
38 K. C. Hultzsch, T. P. Spaniol, and J. Okuda, *Organometallics*, 1997, **16**, 4845-4856.
39 K. C. Hultzsch, T. P. Spaniol, and J. Okuda, *Angew. Chem. Int. Ed.*, 1999, **38**, 227-230.
40 Z.-M. Hou, Y.-G. Zhang, H. Tezuka, P. Xie, O. Tardif, T. A. Koizumi, H. Yamazaki, and Y. Wakatsuki, *J. Am. Chem. Soc.*, 2000, **122**, 10533-10543.
41 Y. Luo, J. Baldamus, and Z. Hou, *J. Am. Chem. Soc.*, 2004, **126**, 13910-13911.
42 A.-S. Rodrigues, E. Kirillov, C. W. Lehmann, T. Roisnel, B. Vuillemin, A. Razavi, and J.-F. Carpentier, *Chem. Eur. J.*, 2007, **13**, 5548-5565.
43 S. Zhou, S. Wang, E. Sheng, L. Zhang, Z. Yu, X. Xi, G. Chen, W. Luo, and Y. Li, *Eur. J. Inorg. Chem.*, 2007, 1519-1528.
44 S. Wang, X. Tang, A. Vega, J.-Y. Saillard, S. Zhou, G. Yang, W. Yao, and Y. Wei, *Organometallics*, 2007, **26**, 1512-1522.
45 K. R. D. Johnson and P. G. Hayes, *Chem. Soc. Rev.*, 2013, **42**, 1947-1960.
46 F. T. Edelmann, D. M. M. Freckmann, and H. Schumann, *Chem. Rev.*, 2002, **102**, 1851-1896.
47 W. E. Piers and D. J. H. Emslie, *Coord. Chem. Rev.*, 2002, **233-234**, 131-155.
48 C. Pi, Z. Zhang, R. Liu, L. Weng, Z. Chen, and X. Zhou, *Organometallics*, 2006, **25**, 5165-5172.
49 K. R. D. Johnson and P. G. Hayes, *Organometallics*, 2009, **28**, 6352-6361.
50 K. R. D. Johnson and P. G. Hayes, *Organometallics*, 2011, **30**, 58-67.
51 K. R. D. Johnson and P. G. Hayes, *Organometallics*, 2013, **32**, 4046-4049.
52 K. R. D. Johnson and P. G. Hayes, *Dalton Trans.*, 2014, **43**, 2448-2457.
53 K. R. D. Johnson, Ph.D. Thesis, University of Lethbridge, 2012.
54 J. J. Eisch and W. C. Kaska, *J. Am. Chem. Soc.*, 1962, **84**, 1501-1502.
55 J. J. Eisch and W. C. Kaska, *J. Organomet. Chem.*, 1964, **2**, 184-187.
56 H. A. Mayer and W. C. Kaska, *Chem. Ber.*, 1990, **123**, 1827-1831.
57 K. R. D. Johnson, M. A. Hannon, J. S. Ritch, and P. G. Hayes, *Dalton Trans.*, 2012, **41**, 7873-7875.
58 R. D. Shannon, *Acta Crystallogr., Sect. A: Found. Crystallogr.*, 1976, **32**, 751-767.
59 W. J. Evans, *Inorg. Chem.*, 2007, **46**, 3435-3449.
60 K. C. Hultzsch, P. Voth, K. Beckerle, T. P. Spaniol, and J. Okuda, *Organometallics*, 2000, **19**, 228-243.
61 W. J. Evans, J. C. Brady, and J. W. Ziller, *J. Am. Chem. Soc.*, 2001, **123**, 7711-7712.
62 M. F. Lappert and R. Pearce, *J. Chem. Soc., Chem. Commun.*, 1973, 126-126.
63 An analysis of 101 entries in the Cambridge Structural Database (CSD version 5.35, updated Nov. 2013) for neutral (trimethylsilyl)methyl yttrium complexes of the generic form $L_nY^{III}(CH_2SiMe_3)_x$ suggested an average $Y–CH_2SiMe_3$ bond length of 2.415 Å (range = 2.339–2.476 Å).
64 M. Shibasaki and N. Yoshikawa, *Chem. Rev.*, 2002, **102**, 2187-2209.
65 H. Schumann, D. M. M. Freckmann, and S. Dechert, *Z. Anorg. Allg. Chem.*, 2002, **628**, 2422-2426.
66 in *Magnetochemistry*, ed. R. L. Carlin, Springer-Verlag, New York, USA, 1986, Chapt. 9.
67 K. D. Conroy, W. E. Piers, and M. Parvez, *J. Organomet. Chem.*, 2008, **693**, 834-846.
68 D. Barbier-Baudry, F. Bonnet, B. Domenichini, A. Dormond, and M. Visseaux, *J. Organomet. Chem.*, 2002, **647**, 167-179.
69 Y. Satoh, N. Ikitake, Y. Nakayama, S. Okuno, and H. Yasuda, *J. Organomet. Chem.*, 2003, **667**, 42-52.
70 D. Baudry, A. Dormond, B. Lachot, M. Visseaux, and G. Zucchi, *J. Organomet. Chem.*, 1997, **547**, 157-165.
71 H. Schumann, M. R. Keitsch, J. Demtschuk, and G. A. Molander, *J. Organomet. Chem.*, 1999, **582**, 70-82.
72 H. Schumann, M. R. Keitsch, and S. H. Mühle, *Z. Anorg. Allg. Chem.*, 2002, **628**, 1311-1318.
73 A. Venugopal, I. Kamps, D. Bojer, R. J. F. Berger, A. Mix, A. Willner, B. Neumann, H.-G. Stammler, and N. W. Mitzel, *Dalton Trans.*, 2009, 5755-5765.
74 W. J. Evans, J. M. Perotti, and J. W. Ziller, *J. Am. Chem. Soc.*, 2005, **127**, 3894-3909.
75 J. C. Gordon, G. R. Giesbrecht, D. L. Clark, P. J. Hay, D. W. Keogh, R. Poli, B. L. Scott, and J. G. Watkin, *Organometallics*, 2002, **21**, 4726-4734.
76 T. Dubé, S. Gambarotta, and G. P. A. Yap, *Organometallics*, 2000, **19**, 817-823.
77 J.-I. Song and S. Gambarotta, *Angew. Chem. Int. Ed. Engl.*, 1995, **34**, 2141-2143.
78 M. N. Bochkarev, V. V. Khramenkov, Y. F. Rad'kov, and L. N. Zakharov, *J. Organomet. Chem.*, 1991, **421**, 29-38.
79 W.-X. Zhang, Z. Wang, M. Nishiura, Z. Xi, and Z. Hou, *J. Am. Chem. Soc.*, 2011, **133**, 5712-5715.
80 E. Lu, Y. Li, and Y. Chen, *Chem. Commun.*, 2010, **46**, 4469-4471.
81 W. Rong, J. Cheng, Z. Mou, H. Xie, and D. Cui, *Organometallics*, 2013, **32**, 5523-5529.
82 B. V. Mork and T. D. Tilley, *J. Am. Chem. Soc.*, 2004, **126**, 4375-4385.
83 Despite exhaustive efforts the elemental analysis data for complex **3** was not satisfactory; the best values from repeated runs are given.
84 S.-H. Wu, Z.-B. Ding, and X.-J. Li, *Polyhedron*, 1994, **18**, 2679-2681.
85 G. B. Deacon, T. Feng, S. Nickel, B. W. Skelton, and A. H. White, *J. Chem. Soc., Chem. Commun.*, 1993, 1328-1329.
86 *APEX2*, (2010) Bruker AXS, Madison, WI.
87 *SAINT-Plus*, (2009) Bruker AXS, Madison, WI.
88 G. M. Sheldrick, *SADABS*, (2008) Bruker AXS, Madison, WI.
89 A. L. Spek, *J. Appl. Cryst.*, 2003, **36**, 7-13.
90 O. V. Dolomanov, J. Bourhis, R. J. Gildea, J. A. K. Howard, and H. Puschmann, *J. Appl. Cryst.*, 2009, **42**, 339-341.

Graphical Abstract

Differences in the cyclometalation reactivity of bisphosphinimine-supported organo-rare earth complexes

Matthew T. Zamora, Kevin R.D. Johnson, Mikko M. Hänninen, and Paul G. Hayes*

A novel yttrium complex [$L_nY(CH_2SiMe_3)_2$] is resistant to cyclometalation, while samarium variants undergo C–H activation, forming unique cyclometalated motifs.

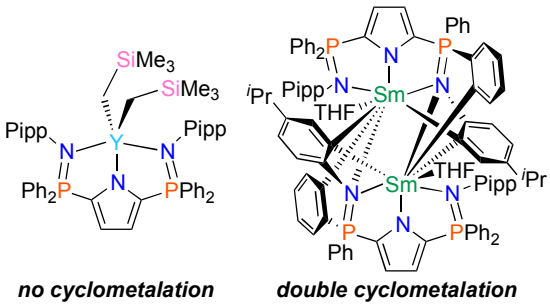

no cyclometalation ***double cyclometalation***